U/Pb LA–ICP–MS age of metamorphic–metasomatic perovskite from serpentinized harzburgite in the Meliata Unit at Dobšiná, Slovakia: Time constraint of fluid–rock interaction in an accretionary wedge

Marián Putiš[1], Yue-Heng Yang[2], Matúš Koppa[1], Marian Dyda[1] & Peter Šmál[1]

[1] Department of Mineralogy and Petrology, Faculty of Natural Sciences, Comenius University in Bratislava, Mlynská dolina, Ilkovičova 6, 842 15 Bratislava, Slovakia; putis@fns.uniba.sk
[2] State Key Laboratory of Lithospheric Evolution, Institute of Geology and Geophysics, Chinese Academy of Sciences, Beijing 100029, China

AGEOS

U/Pb vek metamorfno-metasomatického perovskitu zo serpentinizovaného harzburgitu meliatskej jednotky pri Dobšinej metódou LA-ICP-MS: časový indikátor interakcie horniny a fluida v akrečnej prizme

Abstract: Perovskite-bearing harzburgites were discovered in a blueschist-bearing mélange complex in the Slovak Inner Western Carpathian Meliata tectonic unit at Dobšiná. Perovskite (1) exclusively occurs in serpentinized parts of harzburgite blocks, while perovskite (2) was found in rodingite veins crosscutting serpentinites. We separated metamorphic–metasomatic perovskite (1) from serpentinized orthopyroxene porphyroclasts of a harzburgite serpentinite in order to date fluid–rock interactions during serpentinization and/or rodingitization by in situ U/Pb LA–ICP–MS, and to compare its age with published ages (from 137±1 Ma to 135±1 Ma, with a mean age of 135.6±0.58 Ma) by U/Pb SIMS from the same locality. Perovskite (1) age at ~135±2.0 Ma was determined in the serpentinized zone of the harzburgite by LA–ICP–MS. Perovskite (2) from a rodingite vein was unsuitable for dating by this method because of its very low U content and general high common lead content. The perovskite (1) age is interpreted to record the interaction of metamorphic fluids with harzburgite fragments in the Neotethyan Meliatic accretionary wedge. Since perovskite (1) is younger than the high-pressure metamorphism of this wedge dated at 160–150 Ma, it constrains the exhumation period of the harzburgite fragments at ca. 135 Ma that is compatible with ages of ~137–135 Ma by U/Pb SIMS.

Key words: perovskite U/Pb LA–ICP–MS dating, serpentinization, rodingitization, Meliatic accretionary wedge, Inner Western Carpathians, Slovakia

1. INTRODUCTION

Perovskite has been reported in the following: (1) SiO_2-undersaturated magmatic rocks (Currie, 1975; Chakhmouradian & Mitchell, 1997, 2000; Mitchell & Chakhmouradian, 1998; Heaman et al., 2003); (2) skarns (Marincea et al., 2010; Uher et al., 2011) and (3) in medium- to lower-temperature reaction or rodingitization domains in greenschist and blueschist to eclogite facies metamorphic rocks (Müntener & Hermann, 1994; Malvoisin et al., 2012).

Although most geochronological publications have focused on magmatic perovskite from kimberlites, lamprophyres, carbonatites, and other alkaline rocks (Heaman, 1989, 2009; Smith et al., 1989; Ireland et al., 1990; Simonetti et al., 2008; Frei et al., 2008; Yang et al., 2009; Li et al., 2010; Reguir et al., 2010; Wu et al., 2010, 2013), herein, the U/Pb age of a metamorphic–metasomatic perovskite (Putiš et al., 2012) is determined by Laser Ablation Inductively Coupled Plasma Mass Spectrometry (LA–ICP–MS) and compared to published perovskite ages by the U/Pb Secondary Ion Mass Spectrometry (SIMS) from the same locality (Li et al., 2014), both dating serpentinization/rodingitization fluid–rock interaction. Similar perovskite types seem to be suitable constraints of hydration processes in accretionary wedges (Brandon, 2004).

Mineral abbreviations used in text, tables and figures are after Whitney & Evans (2010): Adr = andradite, Chl = chlorite, Cpx = clinopyroxene, Opx = orthopyroxene, Pph = pyrophanite, Prv = perovskite, Spl = spinel, Srp = serpentine group minerals (undistinguished).

2. GEOLOGICAL SETTING AND REVIEW OF GENETIC ASPECTS OF DATED PEROVSKITE

The Western Carpathians form a collisional orogenic belt subdivided into Outer, Central, and Inner Western Carpathians (OWC, CWC and IWC – Plašienka et al., 1997, Fig. 1); where

Manuscript received 18 July 2014
Revised version accepted 23 January 2015

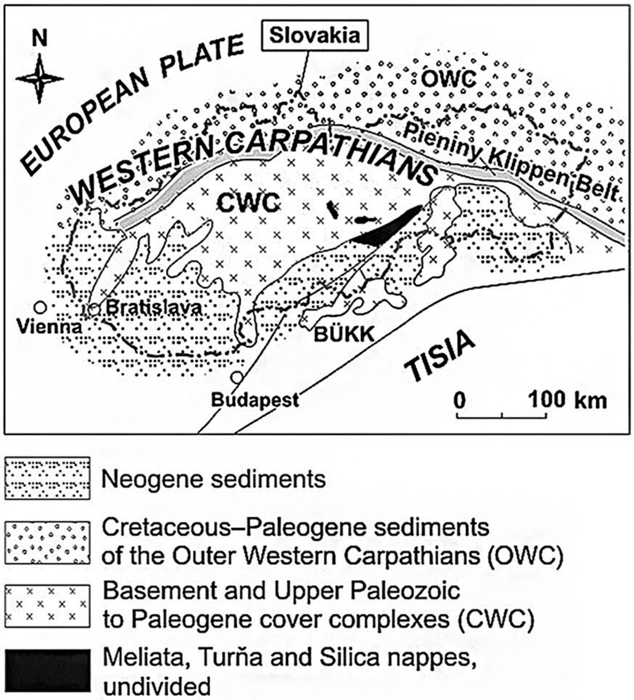

Fig. 1. Geological-tectonic sketch map of Pre-Cenozoic units of the Western Carpathians (after Biely et al., 1996). OWC = Outer Western Carpathians; CWC = Central Western Carpathians, divided into the Tatric, Veporic and Gemeric basement–cover complexes (Late Cretaceous tectonic units) overlain by small (often less than kilometer size) fragments of the Meliata tectonic Unit. IWC = Inner Western Carpathians.

Obr. 1 Geologicko-tektonická skica predkenozoických jednotiek Západných Karpát (podľa Bieleho et al., 1996). OWC = vonkajšie Západné Karpaty; CWC = centrálne Západné Karpaty, rozdelené na komplexy fundamentu a obalu tatrika, veporika a gemerika (vrchnokriedové tektonické jednotky) prekryté príkrovovými fragmentmi meliatskej tektonickej jednotky; IWC = vnútorné Západné Karpaty.

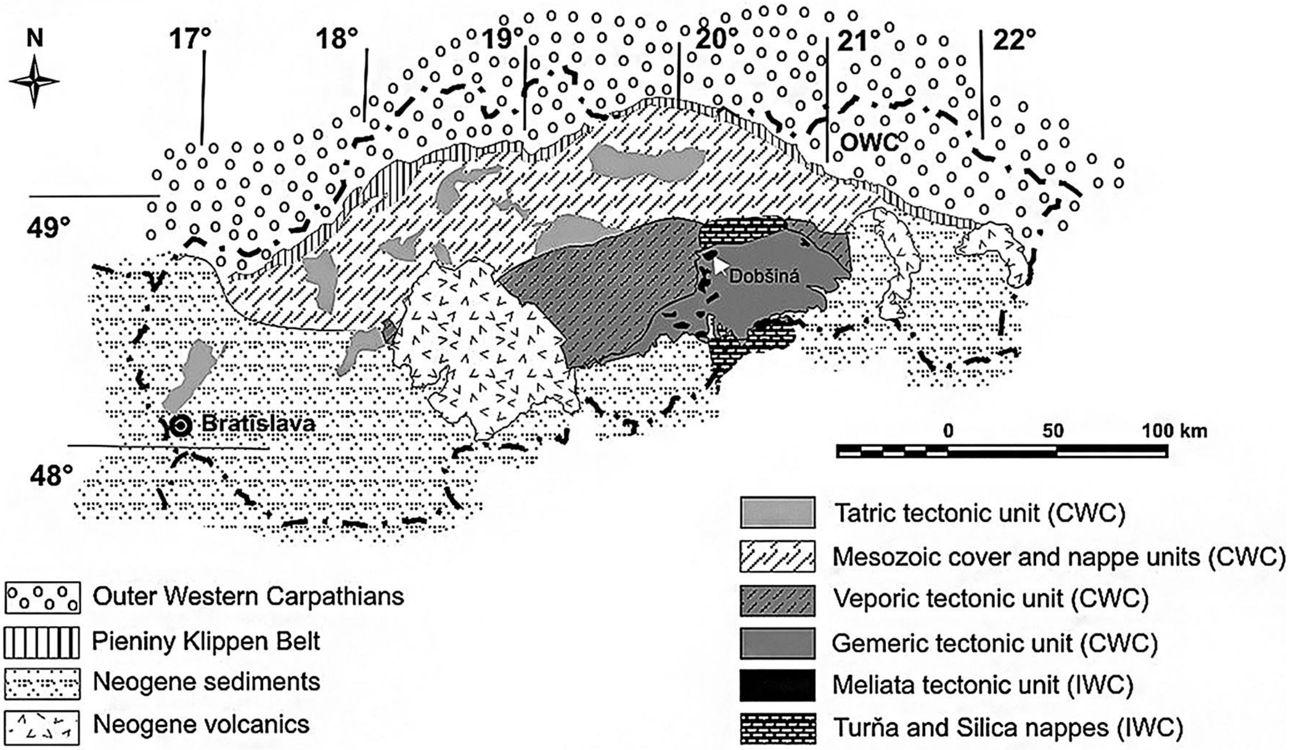

(1) the OWC are mainly composed of Cenozoic flysch complexes, (2) the CWC comprise the basement and Mesozoic cover nappes exposed in the Tatric, Veporic, and Gemeric tectonic zones separated by major Late Cretaceous shear zones (Fig. 1), and (3) the IWC include the Meliata tectonic unit overlain by the Turňa and Silica nappes thrust over the CWC Gemeric Unit (Fig. 1).

The dated Meliatic Bôrka Nappe perovskite-bearing serpentinites associated with blueschist facies rocks are located in the serpentinite quarry at Dobšiná township in eastern Slovakia (Putiš et al. 2011, 2012; Figs 1, 2). Radvanec (2009) discovered perovskite in a pale fragment enclosed in serpentinites at the Danková locality, close to Dobšiná and considered that Prv is most likely a product of ultra-high-pressure metamorphism. Putiš et al. (2012) published geological, mineralogical–petrological, whole-rock chemical data and a preliminary genetic model for perovskite and its harzburgite host. These authors

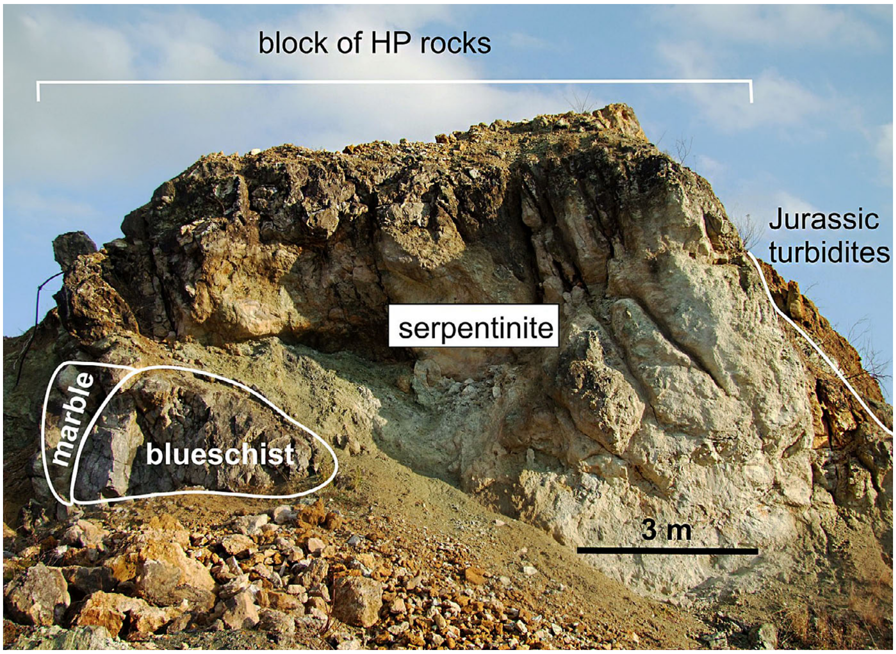

Fig. 2. The mélange complex of the Meliata (IWC) tectonic unit in the Dobšiná quarry, Slovakia.
Obr. 2 Melanž meliatskej (IWC) tektonickej jednotky v dobšinskom kameňolome, Slovensko.

proposed a late-metamorphic/metasomatic origin for Prv related to serpentinization and rodingitization in a subduction–accretionary wedge. Zajzon et al. (2013) described Prv replaced by Pph in Perkupa serpentinite in northern Hungary. Li et al. (2014) reported perovskite genesis related to accretionary wedge serpentinization and rodingitization from the LA–ICP–MS and Laser Ablation Multi-collector Inductively Coupled Plasma Mass Spectrometry (LA–MC–ICP–MS) data, and the U/Pb SIMS dating as well.

The perovskite-bearing serpentinized harzburgite blocks described herein belong to a mélange complex of the Meliata tectonic unit (Putiš et al., 2012). Mock et al. (1998) had previously reported that high-pressure rocks of the Meliata Unit were incorporated in the Bôrka Nappe (Leško & Varga 1980; Mello et al., 1998) overlying the Gemeric and Veporic tectonic units of the CWC. Faryad (1995) specified metamorphic blueschist facies conditions of 380–460 °C at 9–12 kbar. Putiš et al. (2012) and Li et al. (2014) estimated temperature of ca. 450–350 °C at high- to medium pressure for the Prv formation.

The mélange complex is composed of talc–"phengite"–glaucophane schists, "phengite" schists, marbles, blueschists of magmatic and sedimentary origin, serpentinites and blueschist facies tectonoclastics (Fig. 2). These occur as decimetre- to 100 metre-size fragments enclosed in a soft serpentinitic matrix, emplaced into Late Jurassic anchimetamorphosed laminated turbiditic flysch sediments.

The Meliata–Hallstatt Ocean opened in Anisian–Ladinian time (Kozur, 1991), most likely as a back-arc basin (Stampfli, 1996). The Late Jurassic closure of this basin was dated at 160–150 Ma by the $^{40}Ar/^{39}Ar$ ages of "phengitic" white mica in the blueschists (Dallmeyer et al., 1996; Faryad and Henjes-Kunst, 1997). The Meliatic accretionary wedge developed during exhumation of blueschist facies rocks from a subduction channel via a corner flow triggered by the leading edge of the upper plate (Putiš et al., 2014). It is considered that the Meliatic accretionary wedge was then transformed between ca. 150 and 130 Ma into numerous small nappe fragments coalescing as the Bôrka Nappe and thrust over the CWC orogenic wedge. This time interval is well documented by K/Ar ages of newly-formed white mica (Árkai et al., 2003) and (U-Th)/He thermochronology (Putiš et al., 2014).

Concerning the genetic aspects, dated Prv (1) does not occur in magmatic mineral assemblages of harzburgite blocks composed of Ol, Opx, Spl, and rare Cpx. Despite Prv (1) can have lamellar-cube shape (Putiš et al., 2011) it was not found as a late magmatic exsolution phase beside Cpx exsolution lamellae in porphyroclastic Opx_1. In case of considered potential magmatic origin, Prv would have most likely subjected to dissolution, similar to magmatic Opx_1 by the effect of Ca-, Ti- (and LREE-Ce,La) – poor aqueous serpentinization fluids, as a potential source of Ca and Ti for evolving rodingitization. Investigated Prv does not belong to HP metamorphic assemblage, the latter registered exclusively from the harzburgite "cores". However, the "cores" are good indicator of Prv (1) in neighbouring narrow zone between Prv-free "cores" and serpentinized harzburgite rims (Putiš et al., 2012; Li et al., 2014). It is interesting that rare Cpx_1 porphyroclasts and Cpx_2 aggregates in harzburgites, or Cpx-rich aggregates in rare lherzolites and clinopyroxenites were much more resistant to serpentinization, what explains missing Prv in these hydrated rocks. Clinopyroxene exsolution lamellae in Opx_1 porphyroclasts of a harzburgite could have been source of Ca and Ti in dissoluting Opx_1 for ingrowing Prv (1). Clinopyroxene became a source of Ca and Ti in an advanced rodingitization stage by the effect of CO_2-rich aqueous fluids, however not for Prv, but directly for (Ti-) Adr crystallization. The best evidence of this process is pseudomorphic replacement of Prv and/or Cpx by Adr aggregates in rare lherzolites and pyroxenites.

Major element compositions of dated Prv were obtained from polished sections using a Cameca SX-100 electron microprobe at the State Geological Institute of Dionýz Štúr in Bratislava (Putiš et al., 2012). Perovskite trace elements detected by LA–ICP–MS are reported by Li et al. (2014). LA–ICP–MS analysis for U/Pb age determination was used also in this paper.

3. MATERIAL AND METHODS

Over 100 grains of perovskite (1) was separated from sample DO-2 Opx porphyroclasts in serpentinized parts of harzburgite fragments (Fig. 3a,b). Perovskite-free dark "cores", with well-preserved original magmatic structures of Spl harzburgite in the serpentinites, were discarded. Perovskite (1) varies in size from 20 to 700 μm and it is present in either lamellar to cubic shape or in crystal aggregates. Meanwhile, Prv (2) was recovered from rodingite veins crosscutting the serpentinites (Fig. 3c,d).

Perovskite presence in our 200 to 300 μm thick rock-slab samples was checked under a Leica DM2500 P microscope at the Comenius University in Bratislava. Perovskite (1) grains, mostly 50 to 300 μm in size, were then handpicked from the samples under a stereomicroscope, embedded in epoxy and polished to expose grain centres.

Perovskites from the Dobšiná serpentinized harzburgites were cast in each epoxy mount with the perovskite Afrikanda (AFK) and Tazheran (TAZ) standards. The ellipsoidal spot was ca. 20 × 30 μm in size and this produced 30–40 μm ablation depths.

U/Pb ages were determined by LA–ICP–MS at the State Key Laboratory of Lithospheric Evolution at the Chinese Academy of Sciences in Beijing, employing analytical procedures from Yuan et al. (2004) and Xie et al. (2008). An ArF excimer Geolas CQ system operating at 193 nm with a pulse width of approximately 15 ns was used in laser ablation analysis. Subsequently, 40, 60 μm and larger spot sizes were used in the 2007 updated GeoLas PLUS laser system. This choice depended on the mineral grain-size, and precision was meticulously maintained throughout this procedure. The laser repetition rate was 2–10 Hz depending on signal intensity, with fluency

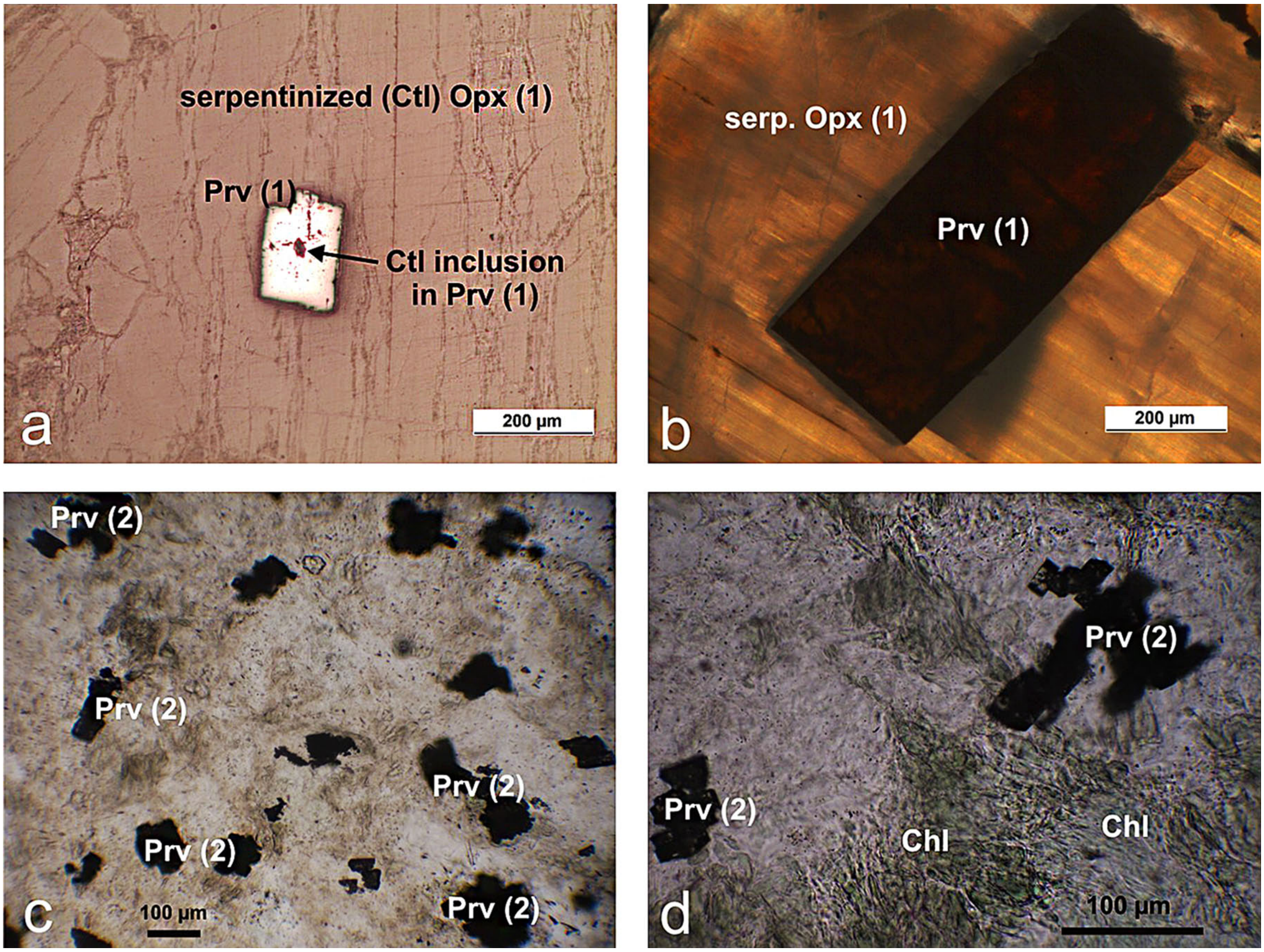

Fig. 3. Microphotographs of perovskite: a – Prv (1) ingrowth in serpentinized (Ctl) Opx porphyroclast from sample DO-2; reflected light image; b – Prv (1) from sample DO-2; polarized light image; c – Prv (2) from sample DO-111; black-wall zone of rodingite vein at contact with host serpentinite; polarized light image; d – Prv (2) from sample DO-111; detail of polarized light image in c.

Obr. 3 Fotografie mikroštruktúr s perovskitom: a – Prv (1) v serpentinizovanom (Ctl) Opx porfyroklaste zo vzorky DO-2. b – Prv (1) zo vzorky DO-2 v polarizovanom svetle. c – Prv (2) zo vzorky DO-111; tmavá reakčná zóna na styku žily rodingitu a okolitého serpentinitu v polarizovanom svetle. d – Prv (2) zo vzorky DO-111; detail obrázku c v polarizovanom svetle.

of ~15 J·cm^{-2}, with ablation depth estimated at ~30–40 μm. With a 40 μm spot size and 4 Hz repetition rate, the volume of ablated material was approximately 200,000 μm^3. Helium gas was then flushed through the sample cell to minimize aerosol deposition around the ablation pit and to improve transport efficiency (Eggins et al., 1998; Jackson et al., 2004). The flow rate of He is usually ca. 0.85 L·min^{-1}.

U/Pb analysis was conducted by Agilent 7500a ICP–MS. During laser ablation, the sensitivity of ^{238}U using NIST SRM 610 standard glass at 40 μm spot and 10 Hz repetition rate was 14,000 cps/ppm. The mass stability was greater than 0.05 amu/24 h; and the ICP–MS detector's Pulse/Analogy (P/A) was corrected prior to routine analysis. A tuning solution optimized instrumental parameters to ensure oxide CeO^+/Ce^+ and doubly charged Ce^{++}/Ce^+ productivity less than 0.5% and 3%, respectively; and also ^{89}Y sensitivity greater than 20×10^6 cps/ppm. The background ^{204}Pb and ^{202}Hg were less than 50 cps resulting from the high purity of employed argon and helium gas.

LA–ICP–MS measurements were performed using time-resolved analysis and peak hopping at one point per mass. The dwell time for each isotope was set at 6 ms for Si, Ca, Ti, Rb, Sr, Ba, Nb, Ta, Zr, Hf and REE, 15 ms for ^{204}Pb, ^{206}Pb, ^{207}Pb and ^{208}Pb and 10 ms for ^{232}Th and ^{238}U. Each 5 sample analysis was followed by one Afrikanda (AFK), Tazheran (TAZ) perovskite and NIST SRM 610 measurement, and each spot analysis consisted of approximately 30 s background and 60 s sample data acquisition. The ^{207}Pb/^{206}Pb, ^{206}Pb/^{238}U, ^{207}Pb/^{235}U (^{238}U/^{235}U = 137.88) and ^{208}Pb/^{232}Th ratios were corrected with IR as external standard. Isotope fractionation was corrected and results were calculated by GLITTER 4.0 (GEMOC, Macquarie University; van Achterbergh et al., 2001), and all measured isotope ratios of standard IR (Ice River) perovskite were regressed during sample analysis and corrected using recommended values, with standard deviations set at 2%. The two stage ^{207}Pb model (Stacey & Kramers, 1975) was applied to make common Pb isotopic ratio corrections (see also Williams, 1998), and the ^{206}Pb/^{238}U weighted mean ages were calculated by ISOPLOT 3.0 (Ludwig, 2003). While individual analysis errors based on counting statistics are at the 1σ level, errors on the pooled ages are quoted at 2σ or 95 % confidence level. Trace element concentrations were calculated using GLITTER 4.0 and calibrated using ^{40}Ca as the internal standard and NIST SRM 610 as external reference. Analytical uncertainties were mostly within 10 %.

4. RESULTS

4.1. In situ LA–ICP–MS analysis of perovskite AFK and TAZ standards for U/Pb dating

AFK perovskite was dated by Wu et al. (2013) from Kola Peninsula alkaline complex. The perovskite U–Pb ages are 377±6 (pyroxenite), 379±5 to 385±5 (calcite-bearing perovskite ore) and 376±5 (ijolite–melteigite) Ma, indicating that this complex formed at ~380 Ma.

Tazheran perovskite from the skarn deposit in the Lake Baikal area of eastern Siberia is used as the U–Pb standard for the Sensitive High Resolution Ion Microprobe (SHRIMP) analysis at Curtin University in Western Australia. Although its chemical composition is unavailable, previous Thermal Ionization Mass Spectrometry (TIMS) analysis indicated that its ^{206}Pb/^{238}U ratio of 0.074465 provides a concordia age of 463 Ma (Kinny et al., 1997). Tazheran perovskite has unusually high U content in excess of 1000 ppm, and chemical analysis highlighted that it consists of relatively pure $CaTiO_3$ with minor amounts of Nb, Fe^{2+} and REE (Ireland et al., 1990; Yang et al., 2009). It has approximately 10 ppm common Pb, with ^{206}Pb/^{204}Pb ratio ranging from 250 to 1000 (Oversby & Ringwood, 1981; Ireland et al., 1990; Kinny et al., 1997). The Isotope Dilution–Thermal Ionization Mass Spectrometry (ID-TIMS) determined TAZ perovskite age at 463 Ma, and its 0.074465 ^{206}Pb/^{238}U ratio is used to standardize SHRIMP measurements (Oversby & Ringwood, 1981; Ireland et al., 1990; Smith et al., 1994; Kinny et al., 1997). However, Kinny et al. (1997) reported that TAZ perovskite has highly variable U and Th concentrations, even within single grains, thus rendering it unsuitable as a concentration standard.

11 U/Pb analyses were conducted on AFK and TAZ standards, respectively, and weighted ^{206}Pb/^{238}U ages of 388.1±5.3 Ma (AFK) and 467.4±5.6 Ma (TAZ) were recorded when the ^{207}Pb correction method was implemented (Fig. 4a–b). These ages are identical, within error, to the recommended values of measured standards.

4.2. Perovskite (1) LA–ICP–MS U/Pb dating

Perovskite (1) from the DO-2 serpentinized harzburgite sample is euhedral, 20–700 μm across, and exhibits almost no alteration. Examples of DO-2 Prv (1) spots dated by LA–ICP–MS are depicted in Fig. 4c. The highest quality crystals were used to measure spots, thus eliminating fractures and inclusions such as Srp, and Ni, Fe, S phases, and also Pph and Adr replacement domains.

Ten DO-2 sample Prv (1) grains (Fig. 4c) from the Dobšiná serpentinized harzburgite were selected for LA–ICP–MS analysis, with twenty-six spots analyzed for U/Pb age determination (Tab. 1). These have high U and Th concentrations and low common Pb concentrations. The ten perovskites have an age of approximately 134.8±2.1 Ma on the concordia Tera-Wasserburg diagram, compatible with a ^{207}Pb corrected age of 135.2±2 Ma (Fig. 4d).

5. DISCUSSION

The perovskite (1) generation from Dobšiná has very low Th concentration and Th/U ratio; very different to magmatic (e.g., Wu et al., 2010) and other reaction–metasomatic (e.g., Yang et al., 2009) perovskites. However, its common Pb is also very low, thus rendering it suitable for precise U/Pb LA–ICP–MS dating. Perovskite (2) grains in DO-111 sample of the Dobšiná rodingites have lower U and Th concentrations and mostly higher common Pb concentrations than Prv (1). It also has variable Th concentrations and Th/U ratios, thus rendering it unsuitable for precise dating.

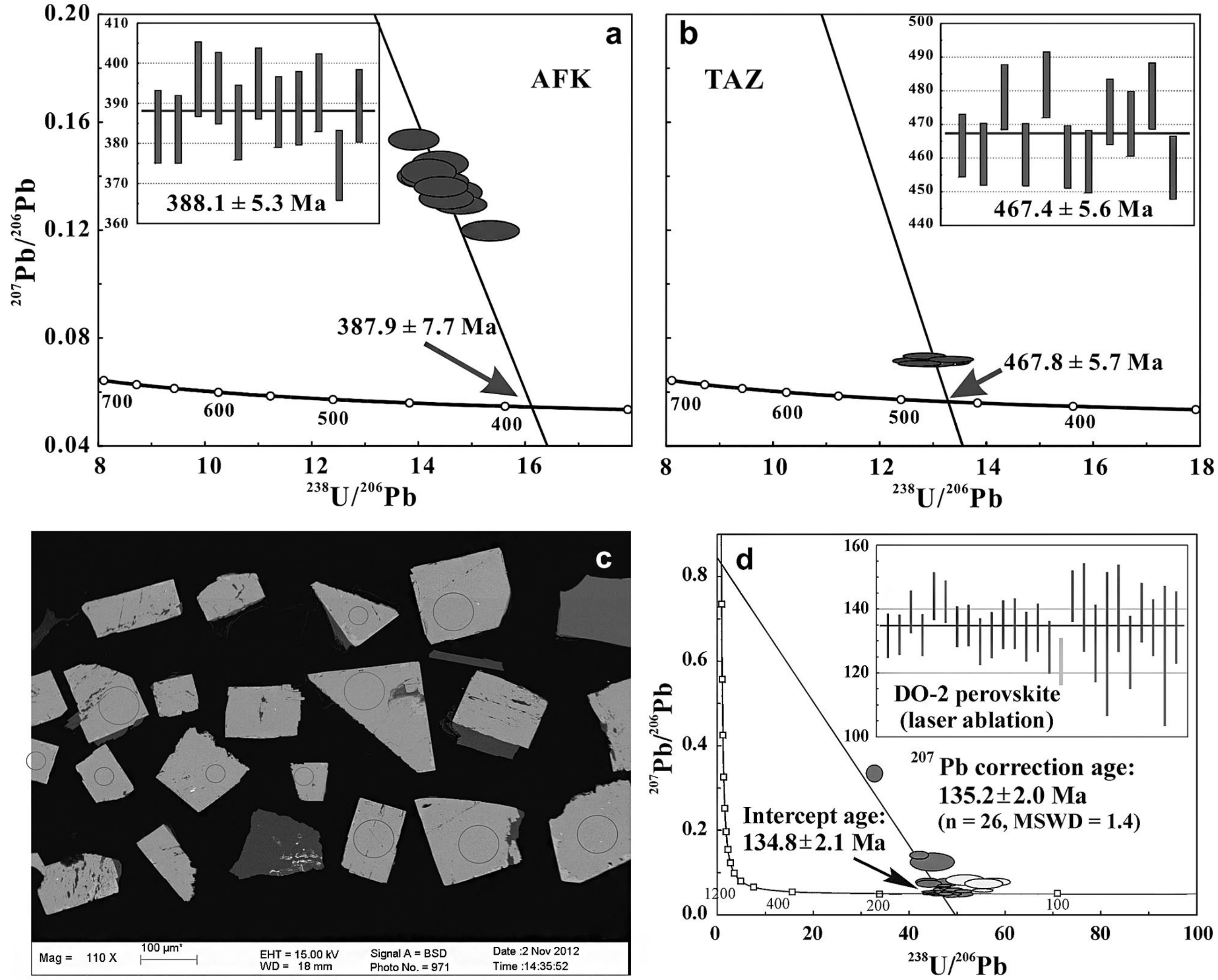

Fig. 4. Concordia Tera-Wasserburg age plot and mean age plot of dated AFK and TAZ perovskite standards, and Dobšiná perovskite (1): a – AFK perovskite standard; b – TAZ perovskite standard; c – Examples of BSE images of dated spots in high-quality fresh Prv (1) from sample DO-2 by LA–ICP–MS. The ellipsoidal 30 and 60 µm spot sizes (or even larger) were used, depending on the mineral grain-size, with similar precision; d – U/Pb LA–ICP–MS plot of concordant and ^{207}Pb corrected ages of Prv (1) from sample DO-2.

Obr. 4 Tera-Wasserburg graf s konkordiou a hlavnými vekmi perovskitových štandardov AFK a TAZ a dobšinského perovskitu (1): a – AFK perovskitový štandard. b – TAZ perovskitový štandard. c – Príklady datovaných (pomocou LA–ICP– MS) bodov nealterovaného Prv (1) zo vzorky DO-2 v spätne rozptýlených elektrónoch. Datované miesta mali tvar elipsy s priemerom 30 a 60 µm (prípadne ešte väčšej) v závislosti od veľkosti zrna Prv, ale datovali sa s rovnakou presnosťou. d – U/Pb LA–ICP– MS graf konkordantného a podľa obsahu ^{207}Pb korigovaného veku Prv (1) zo vzorky DO-2.

The Prv (1) age of ca. 135±2 Ma from LA–ICP–MS analysis is consistent with the inferred post-magmatic, metamorphic–metasomatic origin of Prv bound to serpentinization and/or rodingitization in a subduction-related accretionary wedge (Putiš et al., 2012; Li et al., 2014).

The obtained LA–ICP–MS U/Pb age of Prv (1) is compatible with the U/Pb SIMS ages (from 137±1 Ma to 135±1 Ma, with a mean age of 135.6±0.58 Ma) of the same Prv generation in the Dobšiná Quarry (Li et al., 2014), pointing a suitability of the LA–ICP–MS dating also of this specific metamorphic–metasomatic type of perovskite, first time dated by this method. This age falls into an interval of K/Ar ages of newly-formed white mica dated from this accretionary wedge (Árkai et al., 2003). This age is well consistent also with the low-temperature (U-Th)/He thermochronology reported from this wedge (Putiš et al., 2014).

The Prv (2) age is considered younger because of slightly postponed rodingitization compared to serpentinization; and this is confirmed by petrographic study.

The perovskite (1) age is younger than the 160–150 Ma for "phengitic" white mica from the associated high-pressure rocks of blueschist facies (Dallmeyer et al., 1996). Since Prv is exclusively present in serpentinized and rodingitized harzburgite, the obtained age of approximately 135 Ma indicates concurrent fluid interaction with harzburgite fragments in the accretionary wedge during exhumation-related serpentinization/rodingitization. This date also constrains the earliest Meliatic Nappe

Tab. 1. LA–ICP–MS perovskite (1) U/Pb isotope data (sample DO-2).
Tab. 1. Izotopové údaje U/Pb perovskitu (1) z LA–ICP–MS (vzorka DO-2).

Analysis_#	$^{207}Pb/^{206}Pb$	1s	$^{206}Pb/^{238}U$	1s	$^{207}Pb/^{235}U$	1s	^{207}Corr	1s
DO2-Ae-pt1-4-an1	0.048	0.003	0.020	0.001	0.134	0.007	129.7	3.6
DO2-Ae-pt1-4-an2	0.044	0.002	0.021	0.001	0.123	0.006	131.8	3.6
DO2-Ae-pt1-4-an3	0.054	0.003	0.021	0.001	0.158	0.007	135.1	3.8
DO2-Ae-pt1-4-an4	0.053	0.003	0.021	0.001	0.156	0.008	135.4	3.9
DO2-Ae-pt1-4-an5	0.053	0.003	0.021	0.001	0.151	0.008	131.4	3.9
DO2-Ae-pt1-4-an6	0.049	0.003	0.021	0.001	0.141	0.007	134.1	3.8
DO2-Ae-pt1-4-an7	0.058	0.004	0.020	0.001	0.163	0.009	128	4.1
DO2-Ae-pt1-4-an8	0.055	0.003	0.020	0.001	0.148	0.008	123.6	3.7
DO2-Ae-pt5-7-an1	0.047	0.002	0.022	0.001	0.140	0.005	139.1	3.3
DO2-Ae-pt5-7-an2	0.050	0.002	0.021	0.001	0.144	0.005	131.8	3.2
DO2-Ae-pt5-7-an3	0.053	0.002	0.023	0.001	0.166	0.006	144	3.7
DO2-Ae-pt8-9-an1	0.050	0.002	0.022	0.001	0.152	0.005	142.3	3.3
DO2-Ae-pt8-9-an2	0.048	0.002	0.021	0.001	0.139	0.004	134.4	3.2
DO2-Ae-pt8-9-an3	0.053	0.002	0.021	0.001	0.155	0.005	134.8	3.2
DO2-Ae-pt12-13-an1	0.068	0.003	0.021	0.001	0.199	0.007	131.6	3.5
DO2-Ae-pt12-13-an2	0.062	0.002	0.021	0.001	0.179	0.005	132	3.1
DO2-F1B-pt3-4-an1	0.049	0.003	0.023	0.001	0.153	0.008	144	4
DO2-f2-pt16-17-an1	0.076	0.008	0.023	0.001	0.238	0.024	140.5	6.9
DO2-f2-pt16-17-an2	0.075	0.008	0.021	0.001	0.218	0.021	129.2	6.1
DO2-f2-pt16-17-an3	0.124	0.017	0.022	0.002	0.381	0.045	129	11.2
DO2-f2-pt16-17-an4	0.073	0.007	0.023	0.001	0.228	0.020	140.2	6.8
DO2-F3-pt1-2-an1	0.048	0.006	0.020	0.001	0.131	0.014	126.4	5.7
DO2-F3-pt1-2-an2	0.053	0.004	0.022	0.001	0.161	0.011	138.8	4.6
DO2-F3-pt1-2-an3	0.059	0.004	0.021	0.001	0.175	0.010	134.2	4.4
DO2-F3-pt1-2-an4	0.333	0.016	0.031	0.001	1.405	0.048	125.3	11
DO2-F3-pt1-2-an6	0.140	0.008	0.024	0.001	0.46	0.021	134.2	5.6

overthrusting the CWC orogenic wedge (e.g., Putiš et al., 2009 and references therein).

6. CONCLUSIONS

Very low Th concentration, low Th/U ratios and generally low common lead content make Prv (1) suitable for precise *in situ* LA–ICP–MS U/Pb dating. Moreover, the exactness of this method approaches the U/Pb SIMS results.

The Tera-Wasserburg age of Prv (1) at 134.8±2.1 Ma (and ^{207}Pb corrected age of 135.2±2 Ma) obtained by U/Pb LA–ICP–MS dates the interaction of slab- and accretionary wedge-derived serpentinization/rodingitization fluids with harzburgite blocks during their exhumation from a subduction channel and incorporation in accretionary wedge.

The obtained Early Cretaceous age constrains the earliest age of the Meliatic Bôrka Nappe overthrusting the CWC orogenic wedge.

Acknowledgements: This work was supported by APVV-0081-10 and VEGA-1/0255/11; 1/0079/15 scientific grants (M.P.). Helpful suggestions of Prof. F.Y. Wu (Beijing) during finalization of the manuscript are gratefully acknowledged. We appreciate suggestions of referees Drs. J. Kráľ and T. Vaculovič, and we thank Mr. R. Marshall for reviewing the English content.

7. REFERENCES

Árkai P., Faryad S.W., Vidal O. & Balogh K., 2003: Very low-grade metamorphism of sedimentary rocks of the Meliata unit, Western Carpathians, Slovakia: implications of phyllosilicate characteristics. *International Journal of Earth Sciences (Geologische Rundschau)*, 92, 1, 68–85.

Biely A., Bezák V., Elečko M., Kaličiak M., Konečný V., Lexa J., Mello J., Nemčok J., Potfaj M., Rakús M., Vass D., Vozár J. & Vozárová A., 1996: Geological map of Slovakia, 1:500 000. State Geological Institute of D. Štúr Publishers, Bratislava.

Brandon M.T., 2004: The Cascadia subduction wedge: the role of accretion, uplift, and erosion. *In:* van der Pluijm B.A. & Marshak S. (Eds.): Earth

Structure, An Introduction to Structural Geology and Tectonics. 2nd edition, WCB/McGraw Hill Press, pp. 566–574.

Chakhmouradian A.R. & Mitchell R.H., 1997: Compositional variation of perovskite-group minerals from the carbonatite complexes of the Kola alkaline province, Russia. *The Canadian Mineralogist*, 35, 5, 1293–1310.

Chakhmouradian A.R. & Mitchell R.H., 2000: Occurrence, alteration patterns, and compositional variation of perovskite in kimberlites. *The Canadian Mineralogist,* 38, 4, 975–994.

Currie K.L., 1975: The geology and petrology of the Ice River alkaline complex, British Columbia. *Geological Survey of Canada Bulletin*, 245, 1–68

Dallmeyer R.D., Neubauer F., Handler R., Fritz H., Müller W., Pana D. & Putiš M., 1996: Tectonothermal evolution of the internal Alps and Carpathians: Evidence from $^{40}Ar/^{39}Ar$ mineral and whole-rock data. *Eclogae Geologicae Helvetiae*, 89, 1, 203–227.

Eggins S.M., Kinsley L.P.J. & Shelley J.M.G., 1998: Deposition and element fractionation processes during atmospheric pressure laser sampling for analysis by ICP–MS. *Applied Surface Science*, 127–129, 278–286.

Faryad S.W., 1995: Phase petrology and *P-T* conditions of mafic blueschists from the Meliata unit, West Carpathians, Slovakia. *Journal of Metamorphic Geology*, 13, 6, 701–714.

Faryad S.W. & Henjes-Kunst F., 1997: Petrological and K–Ar and $^{40}Ar–^{39}Ar$ age constraints for the tectonothermal evolution of the high-pressure Meliata unit, Western Carpathians (Slovakia). *Tectonophysics*, 280, 1–2, 141–156.

Frei D., Hutchison M.T., Gerdes A. & Heaman L.M., 2008: Common-lead corrected U–Pb age dating of perovskite by laser ablation - magnetic sectorfield ICP-MS. 9th International Kimberlite Conference Extended Abstract No. 9IKC-A-00216, Frankfurt, Germany.

Heaman L.M., 1989: The nature of the subcontinental mantle from Sr–Nd–Pb isotopic studies on kimberlitic perovskite. *Earth and Planetary Science Letters*, 92, 3–4, 323–334.

Heaman L.M., 2009: The application of U–Pb geochronology to mafic, ultramafic and alkaline rocks: An evaluation of three mineral standards. *Chemical Geology*, 261, 1–2, 43–52.

Heaman L.M., Kjarsgaard B.A. & Creaser R.A., 2003: The timing of kimberlite magmatism in North America: implications for global kimberlite genesis and diamond exploration. *Lithos*, 71, 2–4, 153–184.

Ireland T.R., Compston W., Williams I.S. & Wendt I., 1990: U–Th–Pb systematics of individual perovskite grains from the Allende and Murchison carbonaceous chondrites. *Earth and Planetary Science Letters*, 101, 2–4, 379–387.

Jackson S.E., Pearson N.J., Griffin W.L. & Belousova E.A., 2004: The application of laser ablation-inductively coupled plasma-mass spectrometry to in situ U–Pb zircon geochronology. *Chemical Geology*, 211, 1, 47–69.

Kinny P.D., Griffin B.J., Heaman L.M., Brakhfogel F.F. & Spetsius Z.V., 1997: SHRIMP U–Pb ages of perovskite from Yakutian kimberlites. *Russian Geology and Geophysics*, 38, 97–105.

Kozur H., 1991: The evolution of the Meliata-Hallstatt ocean and its significance for the early evolution of the Eastern Alps and Western Carpathians. *Palaeogeography, Palaeoclimatology, Palaeoecology*, 87, 1–4, 109–135.

Leško B. & Varga I., 1980: Alpine elements in the West Carpathian structure and their significance. *Mineralia Slovaca*, 12, 2, 97–130.

Li Q.L., Li X.H., Liu Y., Wu F.Y., Yang J.H. & Mitchell R.H., 2010: Precise U–Pb and Th–Pb age determination of kimberlitic perovskites by secondary ion mass spectrometry. *Chemical Geology*, 269, 3–4, 396–405.

Li X.H., Putiš M., Yang Y.H., Koppa M. & Dyda M., 2014: Accretionary wedge harzburgite serpentinization and rodingitization constrained by perovskite U/Pb SIMS age, trace elements and Sm/Nd isotopes: Case study from the Western Carpathians, Slovakia. *Lithos*, 205, 1–14.

Ludwig K.R., 2003: ISOPLOT/Ex version 3.0–A Geochronological toolkit for Microsoft Excel. Berkeley Geochronology Center Special Publication, No. 4, 70 p.

Malvoisin B., Chopin Ch., Brunet F. & Galvez M.E., 2012: Low-temperature wollastonite formed by carbonate reduction: a marker of serpentinite redox conditions. *Journal of Petrology*, 53, 1, 159–176.

Marincea Ş., Dumitra Ş.D.G. & Fransolet A.M., 2010: The association spurrite–perovskite in the inner exoskarn zone from Cornet Hill (Metaliferi Mountains, Romania). *Acta Mineralogica-Petrographica, Abstract Series*, 6, 433.

Mello J., Ivanička J. (Eds.), Grecula P., Janočko J., Jacko S. (sen.), Elečko M., Pristaš J., Vass D., Polák M., Vozár J., Vozárová A., Hraško Ľ., Kováčik M., Bezák V., Biely A., Németh Z., Kobulský J., Gazdačko Ľ., Madarás J. & Olšavský M., 2008: General geological map of the Slovak Republic 1:200 000. Map sheet: 37 – Košice. Ministry of the Environment of the Slovak Republic, State Geological Institute of D. Štúr, Bratislava.

Mitchell R.H. & Chakhmouradian A.R., 1998: Instability of perovskite in a CO_2-rich environment; examples from carbonatite and kimberlite. *The Canadian Mineralogist*, 36, 939–952.

Mock R., Sýkora M., Aubrecht R., Ožvoldová L., Kronome B., Reichwalder P. & Jablonský J., 1998: Petrology and petrography of the Meliaticum near the Meliata and Jaklovce Villages, Slovakia. *Slovak Geological Magazine*, 4, 4, 223–260.

Müntener O. & Hermann J., 1994: Titanian andradite in a metapyroxenite layer from the Malenco ultramafics (Italy): implications for Ti-mobility and low oxygen fugacity. *Contributions to Mineralogy and Petrology*, 116, 1–2, 156–168.

Oversby V.M. & Ringwood A.E., 1981: Lead isotopic studies of zirconolite and perovskite and their implications for long range Synroc stability. *Radioactive Waste Management*, 1, 289–307.

Plašienka D., Grecula P., Putiš M., Kováč M. & Hovorka D., 1997: Evolution and structure of the Western Carpathians: an overview. *In:* Grecula P., Hovorka D. & Putiš M. (Eds.): Geological Evolution of the Western Carpathians. Mineralia Slovaca – Geocomplex, Bratislava, pp. 1–24.

Putiš M., Frank W., Plašienka D., Siman P., Sulák M. & Biroň A., 2009: Progradation of the Alpidic Central Western Carpathians orogenic wedge related to two subductions: constrained by $^{40}Ar/^{39}Ar$ ages of white micas. *Geodinamica Acta*, 22, 1–3, 31–56.

Putiš M., Radvanec M., Hain M., Koller F., Koppa M. & Snárska B., 2011: 3-D analysis of perovskite in serpentinite (Dobšiná quarry) by X-ray microtomography. *In:* Ondrejka M. & Šarinová K. (Eds.): Proceedings, Petros Symposium, Bratislava, Comenius University Press, pp. 33–37.

Putiš M., Koppa M., Snárska B., Koller F. & Uher P., 2012: The blueschist-associated perovskite–andradite-bearing serpentinized harzburgite from Dobšiná (the Meliata Unit), Slovakia. *Journal of Geosciences*, 58, 4, 221–240.

Putiš M., Danišík M., Ružička P. & Schmiedt I., 2014: Constraining exhumation pathway in an accretionary wedge by (U-Th)/He thermochronology–Case study on Meliatic nappes in the Western Carpathians. *Journal of Geodynamics*, 81, 80–90.

Radvanec M., 2009: P-T path of perovskite–clinopyroxene–grossular bearing fragments enclosed in meta-peridotite (Danková, Gemer area, Western Carpathians). 8th International Eclogite Conference, Xining, China, Abstracts, 121–122.

Reguir E.P., Camacho A., Yang P., Chakhmouradian A.R., Kamenetsky V.S. & Halden N.M., 2010: Trace-element study and uranium–lead dating of perovskite from the Afrikanda plutonic complex, Kola Peninsula (Russia) using LA-ICP-MS. *Mineralogy and Petrology*, 100, 3–4, 95–103.

Simonetti A., Heaman L.M. & Chacko T., 2008: Use of Discrete-Dynode Secondary Electron Multipliers with Faradays – a 'Reduced Volume' Approach for In-Situ U–Pb Dating of Accessory Minerals Within Petrographic Thin Sections by LA– MC–ICP–MS. *Mineralogical Association of Canada Short Course Series*, 40, pp. 241–264.

Smith C.B., Allsopp H.L., Gravie O.G., Kramers J.D., Jackson P.F.S. & Clement C.R., 1989: Note on the U-Pb perovskite method for dating kimberlites: Examples from Wesselton and De Beers mines, South Africa, and Somerset Island, Canada. *Chemical Geology: Isotope Geoscience section*, 79, 2, 137–145.

Smith C.B., Clark T.C., Barton E.A., & Bristow J.W., 1994: Emplacement ages of kimberlite occurrences in the Prieska region, southwest border of the Kaapvaal Craton, South Africa. *Chemical Geology*, 113, 149–169.

Stacey J.S. & Kramers J.D., 1975: Approximation of terrestrial lead isotope evolution by a two-stage model. *Earth and Planetary Science Letters*, 26, 2, 207–221.

Stampfli G.M., 1996: The Intra-Alpine terrain: A Paleotethyan remnant in the Alpine Variscides. *Eclogae Geologicae Helvetiae*, 89, 1, 13–42.

Uher P., Koděra P. & Vaculovič T., 2011: Perovskite from Ca-Mg skarn-porphyry deposit Vysoká – Zlatno, Štiavnica stratovolcano, Slovakia. *Mineralia Slovaca*, 43, 3, 247–254.

van Achterbergh E., Ryan C., Jackson S. & Griffin W.L., 2001: Appendix 3, data reduction software for LA–ICP–MS. *In:* Sylvester P. (Ed.): Laser-Ablation–ICPMS in the Earth Sciences. *Mineralogical Association of Canada Short Course Series*, 29, pp. 239–243.

Whitney D.L. & Evans B.W., 2010: Abbreviations for names of rock-forming minerals. *American Mineralogist*, 95, 1, 185–187.

Williams I.S., 1998: U–Th–Pb geochronology by ion microprobe. *In:* McKibben M.A., Shanks W.C.P. & Ridley W.I. (Eds.): Applications of Microanalytical Techniques to Understanding Mineralizing Processes. *Reviews in Economic Geology*, 7, 1–35.

Wu F.Y., Yang Y.H., Mitchell R.H., Li Q.L., Yang J.H. & Zhang Y.B., 2010: In situ U–Pb age determination and Nd isotopic analysis of perovskites from kimberlites in southern Africa and Somerset Island, Canada. *Lithos*, 115, 1–4, 205–222.

Wu F.Y., Arzamastsev A.A., Mitchell R.H., Li Q.L., Sun J., Yang Y.H. & Wang R.Ch., 2013: Emplacement age and Sr–Nd isotopic compositions of the Afrikanda alkaline ultramafic complex, Kola Peninsula, Russia. *Chemical Geology*, 353, 210–229.

Xie L.W., Zhang Y.B., Zhang H.H., Sun J.F. & Wu F.Y., 2008: *In situ* simultaneous determination of trace elements, U–Pb and Lu–Hf isotopes in zircon and baddeleyite. *Chinese Science Bulletin*, 53, 10, 1565–1573.

Yang Y.H., Wu F.Y., Wilde S.A., Liu X.-M., Zhang Y.B., Xie L.W. & Yang J.H., 2009: *In situ* perovskite Sr–Nd isotopic constraints on the petrogenesis of the Ordovician Mengyin kimberlites in the North China Craton. *Chemical Geology*, 264, 1–4, 24–42.

Yuan H.L., Gao S., Liu X.M., Li H.M., Gunther D. & Wu F.Y., 2004: Accurate U–Pb age and trace element determinations of zircon by laser ablation–inductively coupled plasma-mass spectrometry. *Geostandards and Geoanalytical Research*, 28, 3, 353–370.

Zajzon N., Váczi T., Fehér B., Takács Á., Szakáll S. & Weiszburg T.G., 2013: Pyrophanite pseudomorphs after perovskite in Perkupa serpentinites (Hungary): a microtextural study and geological implications. *Physics and Chemistry of Minerals*, 40, 8, 611–623.